12th ANKARA INTERNATIONAL AEROSPACE CONFERENCE **AIAC-2023-071**
13-15 September 2023 - Online, Ankara, TURKIYE

# HOMOGENIZATION OF NANOCOMPOSITES WITH AGGLOMERATING NANO-INCLUSIONS USING EMBEDDED ELEMENT METHOD

Alperen Demirtaş* and Ercan Gürses†
Middle East Technical University
Ankara, Turkey

## ABSTRACT

*Nanocomposites are materials that consist of matrix and nano inclusions as reinforcement. Aside aforementioned two phases, nanoparticles can agglomerate and construct a new phase with different mechanical and geometrical properties. This study aims to investigate the mechanical properties of a nanocomposite material by homogenization using the embedded element method considering the agglomeration effect. A representative volume element (RVE) is assembled to achieve this objective, which exhibits the same mechanical properties as the whole nanocomposite material. Elastic constants of the RVE are determined by computing average stresses for several loading cases. The critical contributions of the study are the calculation method of the mechanical properties and the formation of the agglomerations.*

## INTRODUCTION

Composite materials are employed in the industry and the studies due to their superior properties. These materials consist of a matrix and inclusions. While the matrix provides the lightweight, the inclusions are used as reinforcements. Overall mechanical properties of composites are obtained by homogenization procedures. There are several homogenization methods in practice [Kareem et al., 2022]. Some of them are analytical such as mixture rules and self-consistent schemes. However, the aforementioned methods do not include the effect of the interaction between phases and the material's topology [Güzel and Gürses, 2022]. Therefore, the "computational homogenization method" is employed in this study to calculate the elastic coefficients of the nanocomposite material.

In numerous cases, the dispersion of the filler materials is not homogeneous or aligned. In addition, agglomeration phases significantly alter the overall mechanical properties, and this effect should not be ignored. Therefore, this study aims to calculate the homogenized properties of the nanocomposite precisely with the proposed procedure and method. In addition to the main goal, it is aimed to decrease the duration of the homogenization process.

*GRA in Aerospace Engineering Department, Email: demirtas.alperen@metu.edu.tr
†Assoc. Prof. in Aerospace Engineering Department, Email: gurses@metu.edu.tr

### Homogenization of Representative Volume Element

A representative volume element (RVE) is the smallest material sample that shows the same mechanical properties as the whole part, which is a non-homogeneous media that should be homogenized to calculate material properties in this study. If inclusions are uniform and distributed homogenously, a single particle-covered matrix would be enough to take as an RVE. Since randomly distributed particles are the issue in this study, larger RVE with several inclusions should be examined. A study about the convergence of the number of inclusions to observe the effect of the agglomerations on mechanical properties is conducted. The embedded element method will be employed to ease the preprocessing work of complex RVE structures.

### Embedded Element Method

The embedded element method (EEM) is used to lower preprocessing costs, especially in meshing the RVE [Liu et al., 2016]. Meshing the RVE, a cubic geometry with various random nano inclusions is a very time-consuming process. Also, ensuring a fine mesh is another issue to consider. Using EEM, the matrix phase can be meshed with structured elements without taking the nano inclusions into account explicitly. In Figure 1, matrix and inclusion phases that meshed with structured elements can be seen.

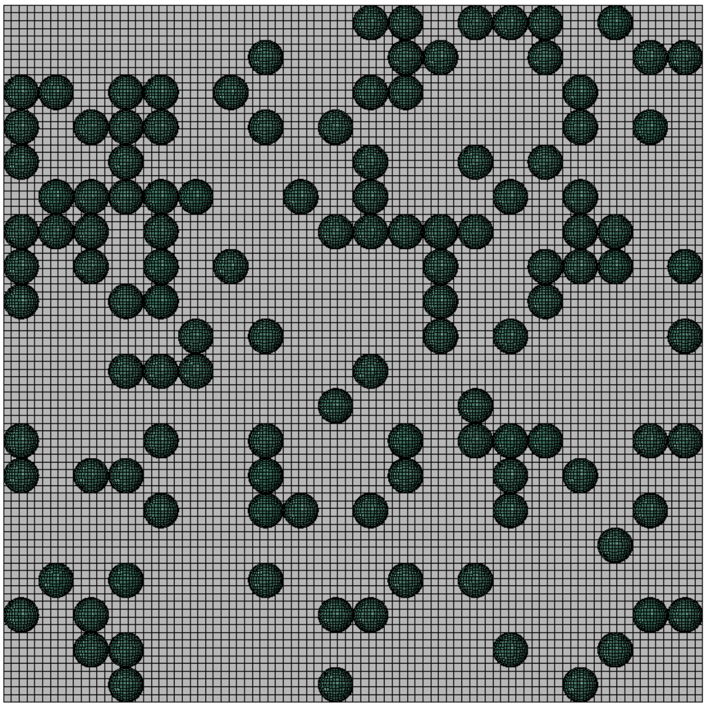

Figure 1: RVE Mesh with Embedded and Host Elements

This method has two element types: host elements and embedded elements. Embedded elements are the inclusion elements, and host elements are matrix elements. Translational degrees of freedom of the nodes belonging to embedded elements are eliminated. The elimination is achieved by constraining the translational degrees of freedom of the embedded nodes to the interpolated values of the nearest nodes of the host elements [ABAQUS, 2014].

## METHOD

Numerous methods can be used to evaluate the bulk properties of a non-homogenous media. These methods can be classified as micromechanics-based approaches such as Mori-Tanaka, the self-consistent scheme; classical bounds as Voigt and Reuss; variational/energy-based methods such as Hashin-Shtrikman bounds; empirical or statistical methods. In this study, finite element-based computational homogenization is used to determine elastic constants.

The computational homogenization method can be explained as follows. Stress and strain values can be obtained from each integration points for each element. In finite element analyses, linear hexagonal elements with full integration are used, each with eight integration points. From these eight integration points, stress, strain, and integration volume values are gathered, and average stress and average strain are computed using the following relations:

$$\boldsymbol{\varepsilon}_{average} = \frac{1}{V}\int \boldsymbol{\varepsilon} dV. \tag{1}$$

$$\boldsymbol{\sigma}_{average} = \frac{1}{V}\int \boldsymbol{\sigma} dV. \tag{2}$$

The integrals in (1) and (2) can be evaluated numerically as sums and the stress and strain tensors can be achieved using the following relations:

$$\bar{\boldsymbol{\sigma}} = \frac{\Sigma_{i=1}^{n}\boldsymbol{\sigma}_i V_i}{\Sigma_{i=1}^{n} V_i}, \tag{3}$$

$$\bar{\boldsymbol{\varepsilon}} = \frac{\Sigma_{i=1}^{n}\boldsymbol{\varepsilon}_i V_i}{\Sigma_{i=1}^{n} V_i}, \tag{4}$$

where $\bar{\boldsymbol{\sigma}}$ and $\bar{\boldsymbol{\varepsilon}}$ are the homogenized stress and strain tensors, $\boldsymbol{\sigma}_i$ and $\boldsymbol{\varepsilon}_i$ are the stress and strain tensors at integration point $i$, $V_i$ is the volume of the integration point $i$ and, $V$ is the total volume of the RVE. Homogenized strain result is calculated to control the result is same with the applied strain.
Stress-strain relations can be used to obtain elasticity tensor as the following:

$$\begin{bmatrix} \sigma_{11} \\ \sigma_{22} \\ \sigma_{33} \\ \sigma_{12} \\ \sigma_{23} \\ \sigma_{13} \end{bmatrix} = \begin{bmatrix} C_{11} & C_{12} & C_{13} & C_{14} & C_{15} & C_{16} \\ & C_{22} & C_{23} & C_{24} & C_{25} & C_{26} \\ & & C_{33} & C_{34} & C_{35} & C_{36} \\ & & & C_{44} & C_{45} & C_{46} \\ & & & & C_{55} & C_{56} \\ sym & & & & & C_{66} \end{bmatrix} \begin{bmatrix} \epsilon_{11} \\ \epsilon_{22} \\ \epsilon_{33} \\ 2\epsilon_{12} \\ 2\epsilon_{23} \\ 2\epsilon_{13} \end{bmatrix} \tag{5}$$

In the most general case, the fourth-order stiffness tensor has 81 components, but this number decreases to 21 independent coefficients due to minor and major symmetries. It further decreases to 9 for orthotropic linear elastic materials. In this case, the stress-strain relation is:

$$\begin{bmatrix} \sigma_{11} \\ \sigma_{22} \\ \sigma_{33} \\ \sigma_{12} \\ \sigma_{23} \\ \sigma_{13} \end{bmatrix} = \begin{bmatrix} C_{11} & C_{12} & C_{13} & 0 & 0 & 0 \\ & C_{22} & C_{23} & 0 & 0 & 0 \\ & & C_{33} & 0 & 0 & 0 \\ & & & C_{44} & 0 & 0 \\ & & & & C_{55} & 0 \\ sym & & & & & C_{66} \end{bmatrix} \begin{bmatrix} \epsilon_{11} \\ \epsilon_{22} \\ \epsilon_{33} \\ 2\epsilon_{12} \\ 2\epsilon_{23} \\ 2\epsilon_{13} \end{bmatrix} \tag{6}$$

As an outcome of this relation, uniaxial tensile and simple shear tests are needed to calculate orthotropic elastic material properties. For an orthotropic material, three tensile and three shear tests are necessary to obtain material properties. In contrast, only one test is sufficient for an isotropic material to obtain Young's modulus and Poisson's ratio. One unidirectional test applies strain only in one direction while restricting others such that:

$$\sigma_1 = C_{11}.\varepsilon_1 + C_{12}.\cancelto{0}{\varepsilon_2} + C_{13}.\cancelto{0}{\varepsilon_3} + C_{14}.\cancelto{0}{\varepsilon_4} + C_{15}.\cancelto{0}{\varepsilon_5} + C_{16}.\cancelto{0}{\varepsilon_6} \tag{7}$$

$$\sigma_1 = C_{11}.\varepsilon_1 \tag{8}$$

**Finite Element Model**

The commercial software package ABAQUS is employed for the modeling of the RVE. Isotropic linear elasticity is assumed for the inclusion and matrix. Elastic constants of the materials are taken from the literature [Demir et al., 2022]. For reinforcement material, Young's modulus is taken as 150 GPa, and for the matrix, the value is 911 MPa. Poisson's ratio is taken as 0.35 for both materials. Material properties of the whole model are computed with displacement-controlled tests. Uniform displacement boundary conditions are applied to the RVE. Mesh quality is an essential factor for the precision of the results. Therefore a mesh study is conducted, and the model is discretized accordingly. RVE that constitutes non-agglomerated particles can be seen in Figure 2.

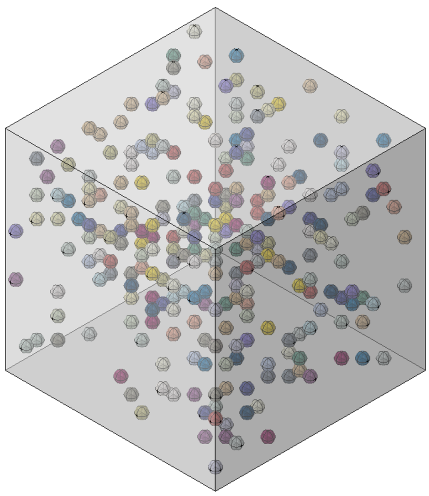

Figure 2: Randomly distributed isolated particles RVE

Agglomerations are formed from randomly distributed particles that are close enough to each other. If the distance between two particles is smaller than a prescribed criterion, an agglomerate (the third phase, i.e., the agglomeration phase) is formed. In that case, particles are removed from the geometry, and a larger sphere (i.e., an agglomerate) that encloses two particles is constructed. Therefore, agglomeration can be treated as larger inclusions with different material properties. The agglomeration phase and non-agglomerated particles can be seen in Figure 3.

Geometries and mechanical properties of the agglomeration phase are calculated before creating the RVE. Different methods can be employed to calculate the elastic coefficients of the agglomerations. The inverse rule of the mixture [Demir et al., 2022], Paul's model [Ma et al., 2017], and other methods are employed in the literature. In this study, the inverse rule of the mixture is employed. The following relation explains the inverse rule of mixture:

$$\frac{1}{E_{agg}} = \frac{v_m}{E_m} + \frac{v_i}{E_i}, \tag{9}$$

$E_{agg}$, $E_m$, and $E_i$ represent Young's modulus of the agglomeration, matrix, and inclusion phases, and $v_m$, and $v_i$ denote the volume fractions of the matrix phase and inclusion phases, respectively. The elastic moduli of the agglomeration phases, including two and three particles, are calculated using 9 as 1212.21 MPa and 1024.10 MPa, respectively.

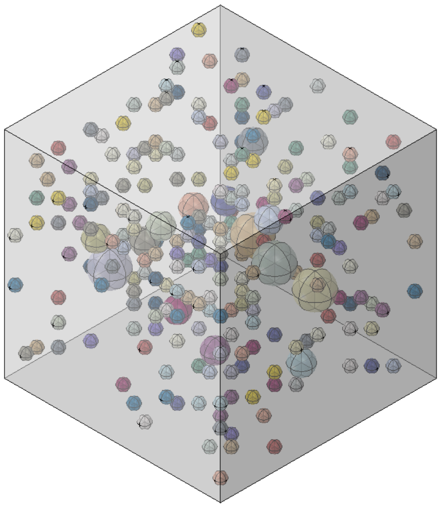

Figure 3: Randomly distributed inclusion RVE with Agglomeration

The effective mechanical properties are calculated in each direction as $E_x$, $E_y$, $E_z$. On the other hand, the average of Young's modulus is taken to compare the results with experiments using the following relation:

$$\bar{E} = \frac{E_x + E_y + E_z}{3} \tag{10}$$

$\bar{E}$ represents the average of the elastic modulus in three directions. Note that since the inclusions are spherical and randomly oriented, the response of the RVE is expected to be almost isotropic.

## RESULTS AND DISCUSSION

The numerical results are presented in this section. At first, a study is conducted to determine the sufficient number of particles to show the agglomeration effect. An RVE is created with respect to the results of the aforementioned convergence study. After that, the homogenized elastic properties are calculated, and two cases, such as well-dispersed particles and agglomerated particles, are compared. Finally, numerical results for different volume fractions are compared with the experimental results from the literature.

### Convergence with Number of Particles

The effect of the agglomerations on mechanical properties can be observed when a sufficient number of particles is loaded in an RVE. Therefore, a minimum number of particles to capture the agglomeration effect should be decided. In order t"o achieve this objective, five different RVEs are created, including different numbers of particles. Two cases of RVEs are created with agglomerated particles and well-dispersed particles. The number of inclusions and effective elastic modulus results are presented in Table 1 and Figure 4.

| # of Inclusions | $E_{agg}$ [GPa] | $E_{iso}$ [MPa] | Difference [%] |
|---|---|---|---|
| 1 | 4.09 | 4.09 | - |
| 6 | 4.09 | 4.09 | - |
| 12 | 4.00 | 4.10 | 2.44 |
| 96 | 3.93 | 4.12 | 4.61 |
| 764 | 3.93 | 4.12 | 4.84 |

Table 1: Results of Convergence with Number of Particles

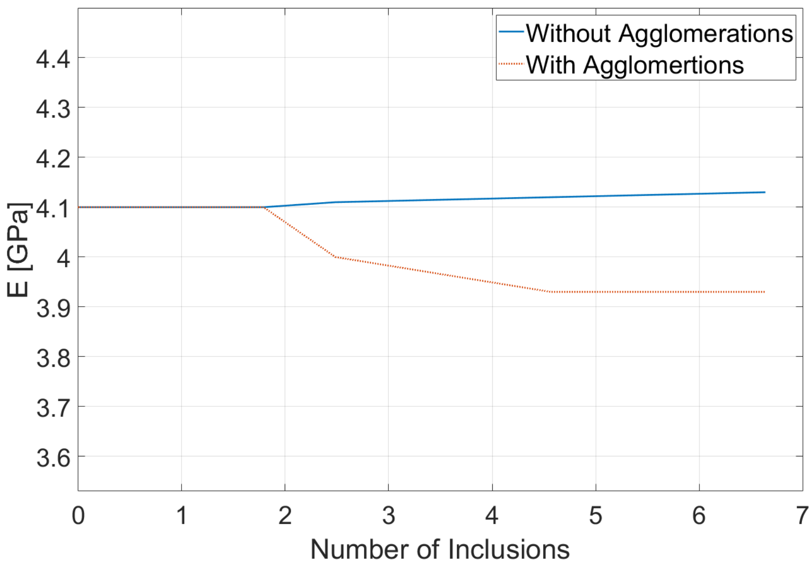


Figure 4: Number of Particles to Observe the Agglomeration Effect

The filler loading is taken as 5% to observe the agglomeration effect clearly. The first two cases, which contain 1 and 6 particles, do not contain any agglomeration phase. On the other hand, the desired difference is obtained after 12 particles. The converged value of the required number of particles is obtained in both 96 and 764 particles. In simulations, filler loading varies between 1 to

10 percent. Therefore, the 764 particle case is determined as the safe case.

### Effect of the Agglomeration on Results

A cubic RVE with an edge length of 10 nm, and the radii of inclusions are 0.25 nm is considered. There are 305 randomly placed nanoparticles leading to 2% of inclusion content. Simple tension and simple shear tests are conducted to RVE using commercial software ABAQUS. The whole model constitutes linear hexagonal elements with full integration. Therefore, each element has eight integration points. As a result of this data set, homogenized properties are calculated, and the results of well-dispersed cases and agglomerated cases are examined. The results of homogenized mechanical properties for the non-agglomerated, well-dispersed case, and agglomerated cases can be seen in Tables 1 and 2, respectively. As seen from the tables, the results are very close to the isotropic response for the well-dispersed and the agglomerated cases.

| $E_x$ [MPa] | $E_y$ [MPa] | $E_z$ [MPa] | $G_{yz}$ [MPa] | $G_{xz}$ [MPa] | $G_{xy}$ [MPa] | $\nu_{yz}$ | $\nu_{xz}$ | $\nu_{xy}$ |
|---|---|---|---|---|---|---|---|---|
| 1030.14 | 1019.37 | 1021.25 | 382.72 | 380.71 | 382.36 | 0.35 | 0.35 | 0.35 |

Table 2: Homogenized mechanical Properties of RVE with no agglomerations

| $E_x$ [MPa] | $E_y$ [MPa] | $E_z$ [MPa] | $G_{yz}$ [MPa] | $G_{xz}$ [MPa] | $G_{xy}$ [MPa] | $\nu_{yz}$ | $\nu_{xz}$ | $\nu_{xy}$ |
|---|---|---|---|---|---|---|---|---|
| 1009.09 | 1004.04 | 1003.37 | 372.68 | 375.61 | 374.52 | 0.35 | 0.35 | 0.35 |

Table 3: Homogenized mechanical Properties of RVE with agglomerations

Furthermore, the Voigt and Reuss bounds for this model can be found using volume fraction and elastic modulus values of the matrix and inclusion materials. The lower bound (Reuss) is calculated as 929.48 MPa, and the upper bound (Voigt) is calculated as 3892.78 MPa for the case that contains non-agglomerated, well-dispersed inclusions. It can be seen that numerical results calculated by using the embedded element method are inside the range. Due to the spherical geometry of the inclusions, the results set are close to the lower bound, as can be predicted. If inclusion geometry is chosen as rod-like geometries, homogenized mechanical properties should be close to the upper bound.

### Comparison with Experiment

A set of results is obtained to compare with the experimental study from the literature [Zamanian et al., 2020]. In this study, silica nanoparticles (Aerosil OX50) are used as reinforcement, and bisphenol A (DGEBA) is used as the matrix material. The average size of the particles is 40 nm, and the average specific surface is 50 $m^2$/g. The volume percentage of the nano-silica content varies between 0.78% to 5.7%. The material properties are taken from the study, and numerical results are obtained accordingly.

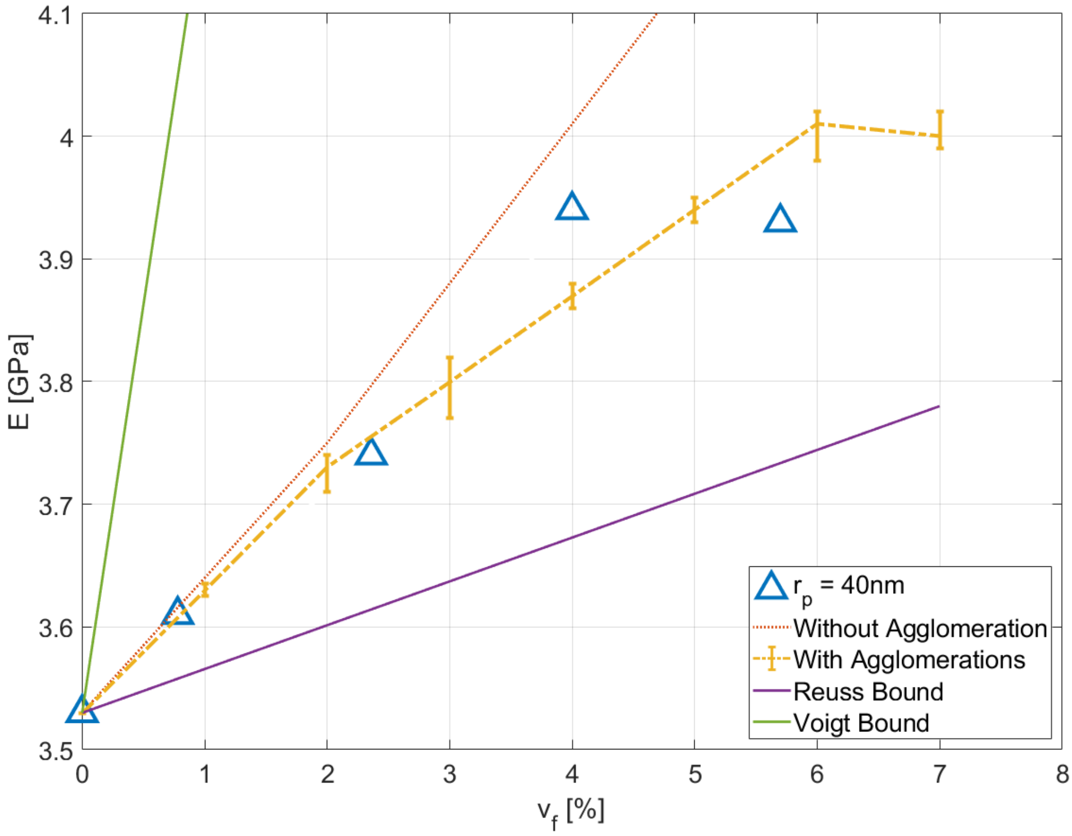


Figure 5: Comparison of the Results with Experiment [Zamanian et al., 2013]

Three different random realizations are generated, and the average of the elastic modulus in each direction for each realization is taken. The average value of Young's modulus is plotted in Figure 5. Also, Reuss and Voigt bounds plotted, as well as the no agglomeration case. The maximum and the minimum values of the elastic moduli results are indicated in the figure also for numerical results. It is observed that both agglomerated and well-dispersed cases are inside the range of the upper and lower bounds. The elastic modulus of the no agglomeration case increases almost linearly with the increasing filler loading. On the other hand, a decrease is observed in the elastic modulus after 6% volume fraction of filler loading when the agglomeration is considered. A similar decrease also can be seen in the experiment.

## CONCLUSIONS

In this study, the effect of the agglomerations on mechanical properties in polymer nanocomposite is investigated. A realistic simulation scenario is prepared for the distribution of the filler materials using the "random sequential adsorption" algorithm [Wang, 1998; Kari et al., 2007]. Therefore, a non-homogenous RVE is created."

The random coordinates of the particles are stored, and two RVEs for two cases are created such that one contains well-dispersed particles while the other one contains agglomerated particles as well as free particles.

Two scripts are developed to detect the agglomerations and to prevent the intersections between particles and agglomerations. Finally, a homogenization script is developed to calculate the elastic coefficients. The result shows that homogenized elastic moduli of the case that includes agglomerated particles are lower than the case that constitutes non-agglomerated, well-dispersed particles; for the same scattering of the inclusions. The effect of the agglomerations on elastic modulus is observed clearly with the increasing filler loading. One critical point is the decrease in Young's modulus after a specific critical volume fraction. The results show that the increased filler loading can result in the degradation of the mechanical property of the nanocomposite. Such a phenomenon is also observed in the literature [Kontou et al., 2006; Ma et al., 2017; Zamanian et al., 2020].

## References

ABAQUS (2014) *ABAQUS/Standard User's Manual Version 6.14* , Dassault Systèmes Simulia Corp, United States, 2014.

Altay, A.E. (2022) *Determination of elastic properties of polymer nanocomposites using embedded element method*, Middle East Technical University, M.Sc. Thesis, 2022.

Demir, E.C., Benkaddour, A., Aldrich, D.R., McDermott, M.T., Kim, I.C. and Ayranci, C. (2022) *A predictive model towards understanding the effect of reinforcement agglomeration on the stiffness of nanocomposites*, Journal of Composite Materials, Vol 56, p: 1591-1604, 2022.

Liu, H., Jiang, L.Y. and Zeng, D. (2016) *Development of RVE-embedded solid elements model for predicting effective elastic constants of discontinuous fiber reinforced composites* ,Mechanics of Materials, Vol 93, p:109-123, 2016.

Ma, X., Zare, Y. and Rhee, K.Y. (2017) *A Two-Step Methodology to Study the Influence of Aggregation/Agglomeration of Nanoparticles on Young's Modulus of Polymer Nanocomposites*, Nanoscale Research Letters 12, 621, 2015.

Zamanian, M., Ghasemi, F. A. and Mortezaei, M. (2020) *Interphase characterization and modeling of tensile modulus in epoxy/silica nanocomposites*, Journal of Applied Polymer Science, Vol 138, 2020.

Zamanian, M., Mortezaei, M., Salehnia, B. and Jam, J.E. (2013) *Fracture toughness of epoxy polymer modified with nanosilica particles: Particle size effect*, Engineering Fracture Mechanics, Vol 93, p: 193-206, 2013.

Kontou, E. and Niaounakis, M. (2006) *Thermo-mechanical properties of LLDPE/SiO2 nanocomposite*, Polymer, Vol 47,p:1267-1280, 2006.

Güzel, D. and Gürses, E. (2022) *A Two-Level Homogenization Approach for Polymer Nanocomposites with Coated Inclusions*, Procedia Structural Integrity, Vol 35,p:34-41, 2022.

Şık, A., Gürses, E. and Sabuncuoğlu, B. (2021) *Development of a procedure to model the mechanical behavior of composites with embedded element method by considering the matrix nonlinearity.*, Composite Structures, Vol 35,p:34-41, 2021.

Kareem, Sarah and Al-Ansari, Luay S and Gömze, László A (2022) *Modeling of modulus of elasticity of nano-composite materials: review and evaluation*, Journal of Physics: Conference Series, IOP Publishing, Vol 2315, 2022.

Wang, J.S. (1998) *Random sequential adsorption, series expansion and Monte Carlo simulation*, Physica A, Vol 254, p:179-184, 1998.

Kari,S., Berger, H., Rodriguez-Ramos, R. and Gabbert, U. (2007) *Computational evaluation of effective material properties of composites reinforced by randomly distributed spherical particles*, Composite Structures, Vol 77, p:223–231, 2007.